Mihir Parikh Donald E. Schreiber

Pattern Partitioning for Enhanced Proximity-Effect Corrections in Electron-Beam Lithography

This paper presents new algorithms for judicious partitioning (or subdivision) of arbitrary lithographic patterns in order to achieve increased quality of proximity-effect correction as well as increased efficiency in the computation of such corrections. Experimental results verifying the correctness of such algorithms are also presented.

Introduction

Proximity effect is a name given to the phenomenon of electron scattering in a resist and substrate leading to undesired exposure in regions adjacent to those addressed by an electron beam. This effect results in incomplete development of some shapes compared to others. The extent of the proximity effect and methods of correcting for it were reviewed in the last issue of this journal [1]. The problem has been alleviated by exposing different shapes in the pattern with different incident electron exposures. This paper presents some new results that show the efficacy of pattern partitioning (or subdivision) for enhanced quality of correction as well as for increased efficiency in the computation of such corrections.

In all of the work to be discussed, we exclusively consider the use of the self-consistent technique [2, 3a]. This technique considers a collection of shapes in a pattern and computes the incident electron exposure such that the influence [1] or resultant exposure (i.e., the sum of the incident plus backscattered electrons) is on the average equal for all shapes in such a collection. For a given pattern, the quality of corrections depends on the number of shapes comprising the input to the algorithm. For example, if the shape is large [4] or if it suffers from large variations in the magnitude of the proximity effect along its periphery, the quality of corrections can be improved [5] by appropriately subdividing the shapes that are sent to the self-consistent algorithm for correction. In the context of different correction algorithms, pattern redefinitions to enhance proximity corrections have been reported [6-8]. Pattern partitioning based on the range of the proximity function has also been proposed [9].

For a given pattern, the computation efficiency of the corrections depends on the number of shapes comprising the input to the self-consistent algorithm. To keep this number as close as possible to an "optimum" value, a zoning technique for an arbitrary pattern has been developed [3b]. For shapes that either traverse or extend significantly beyond the borders of a zone, appropriate subdivision of shapes enhances the quality of correction as well as improves the computation efficiency of correction.

Partitioning for enhanced correction

The quality of corrections attainable with the self-consistent algorithm [3a] is limited by the quality of the pattern data comprising the input to the algorithm. For example, if the letter V is to be written by an electron-beam machine, it can be described by three shapes: two parallelograms and one triangle [Fig. 1(a)]. Subdivision [3c] of each of these shapes [Fig. 1(b)] into, for example, 2n + 1 shapes (where n is the number of vertices) could increase the fidelity of the pattern. However, an increase in the number of shapes (and thus the data volume and computation time) necessitates an intelligent algorithm for partitioning of a pattern only at those locations that are significantly influenced by proximity effects. Such an algorithm has been proposed elsewhere [5]; we present here an implementation.

Copyright 1980 by International Business Machines Corporation. Copying is permitted without payment of royalty provided that (1) each reproduction is done without alteration and (2) the *Journal* reference and IBM copyright notice are included on the first page. The title and abstract may be used without further permission in computer-based and other information-service systems. Permission to *republish* other excerpts should be obtained from the Editor.

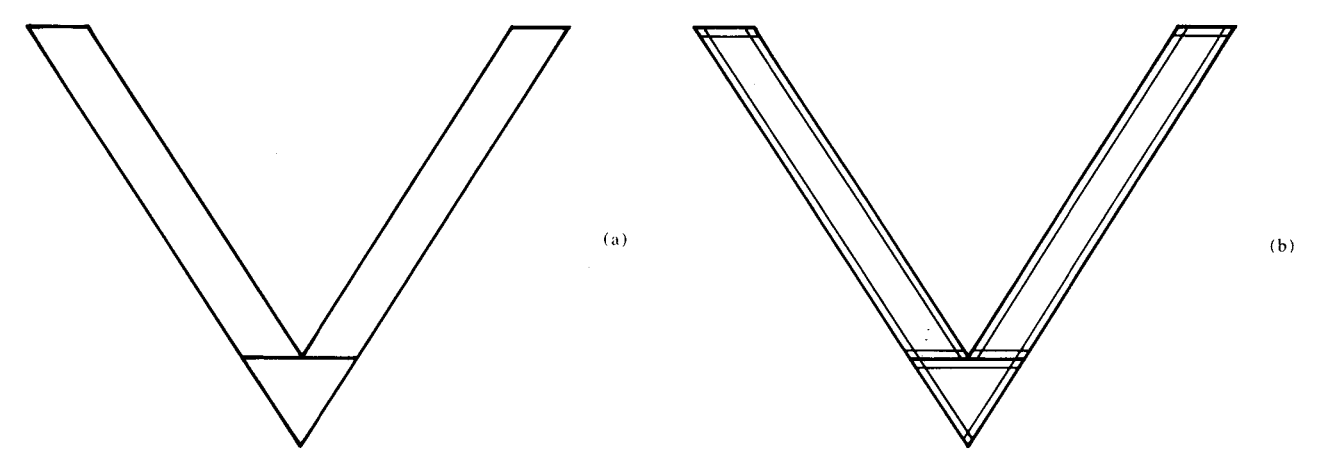


Figure 1 Subdivision of a complex shape into (a) two parallelograms and one triangle, and (b) 25 shapes. In the latter case, increased pattern delineation can be obtained by exposing the edge and corners of shapes with different incident electron exposures as determined using the self-consistent algorithm (reprinted with permission from Ref. [3c]).

Consider the pattern defined by eight rectangular shapes, as shown in Fig. 2. The lithographic pattern that results after exposure of a 0.6-\mum-thick PMMA resist on a silicon substrate by a 20-keV ($\approx 3 \times 10^{-15}$ J) e-beam in our Vector-Scan (VS) electron lithography machine [10] is shown in Fig. 3(a). This pattern, hereafter called the uncorrected pattern, was written with the same exposure $(\approx 80 \mu \text{C/cm}^2)$ throughout all of the eight rectangles in the pattern. The problem caused by the proximity effect is clearly evident. While the regions within the large rectangles are developed to completion, the narrow 1- μ m lines [see regions A and C in Fig. 3(a)] show a significant amount of underdevelopment in terms of resist residue. Further development would decrease the narrow gap between the large shapes (region D), making the pattern unacceptable. A significant alleviation of this problem is achieved through the use of the self-consistent technique [3a]. The normalized incident electron exposure values calculated for the eight rectangles are noted in Fig. 2. Figure 3(b) shows the pattern in the resist after such a correction. Development conditions (using stabilized roomtemperature developer consisting of 1:1 methylisobutylketone and isopropyl alcohol) and criteria used here are of the type reported previously [3c]. While all regions of the pattern have been developed to completion, two regions suffer from problems due to intershape proximity effect. These are evident in region C in Fig. 3(b) as a slight bulging of the 1- μ m line in the vicinity of the 2- μ m-wide rectangle. Also, the resist gap between the large shapes suffers from significant curvature (see region D). Both of these problems can be attributed to the fact that only eight rectangles were submitted to the selfconsistent technique for correction, thereby yielding only

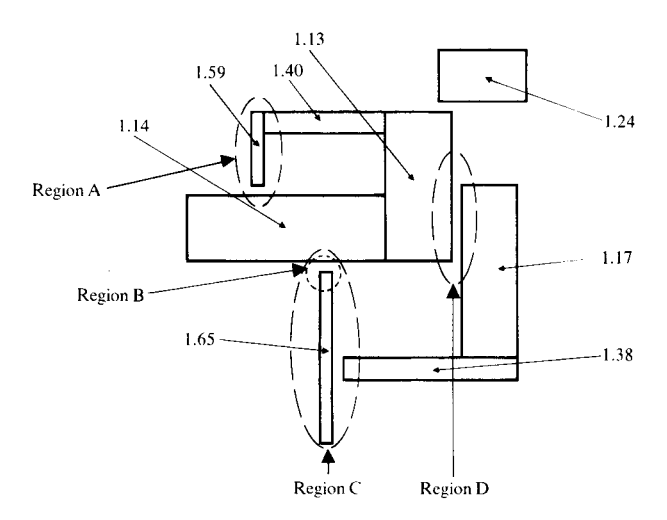


Figure 2 A pattern consisting of eight rectangles. Note regions where proximity corrections are necessary for complete dissolution of the resist as well as pattern fidelity. If this pattern is not proximity-corrected, a relative incident electron exposure value of unity is given to each rectangle. If this pattern is corrected via the self-consistent algorithm, incident electron exposure values are given to each rectangle as noted.

average values for the long 1- μ m rectangle (see region C) and the two large rectangles (region D) on either side of the gap. Such average values are clearly inadequate for complete proximity correction. Intelligent subdivision or partitioning of such shapes and subsequent recomputation of corrections can be expected to correct such problems [5].

The strategy for partitioning the pattern (see Fig. 4) in order to optimize the quality of corrections attainable

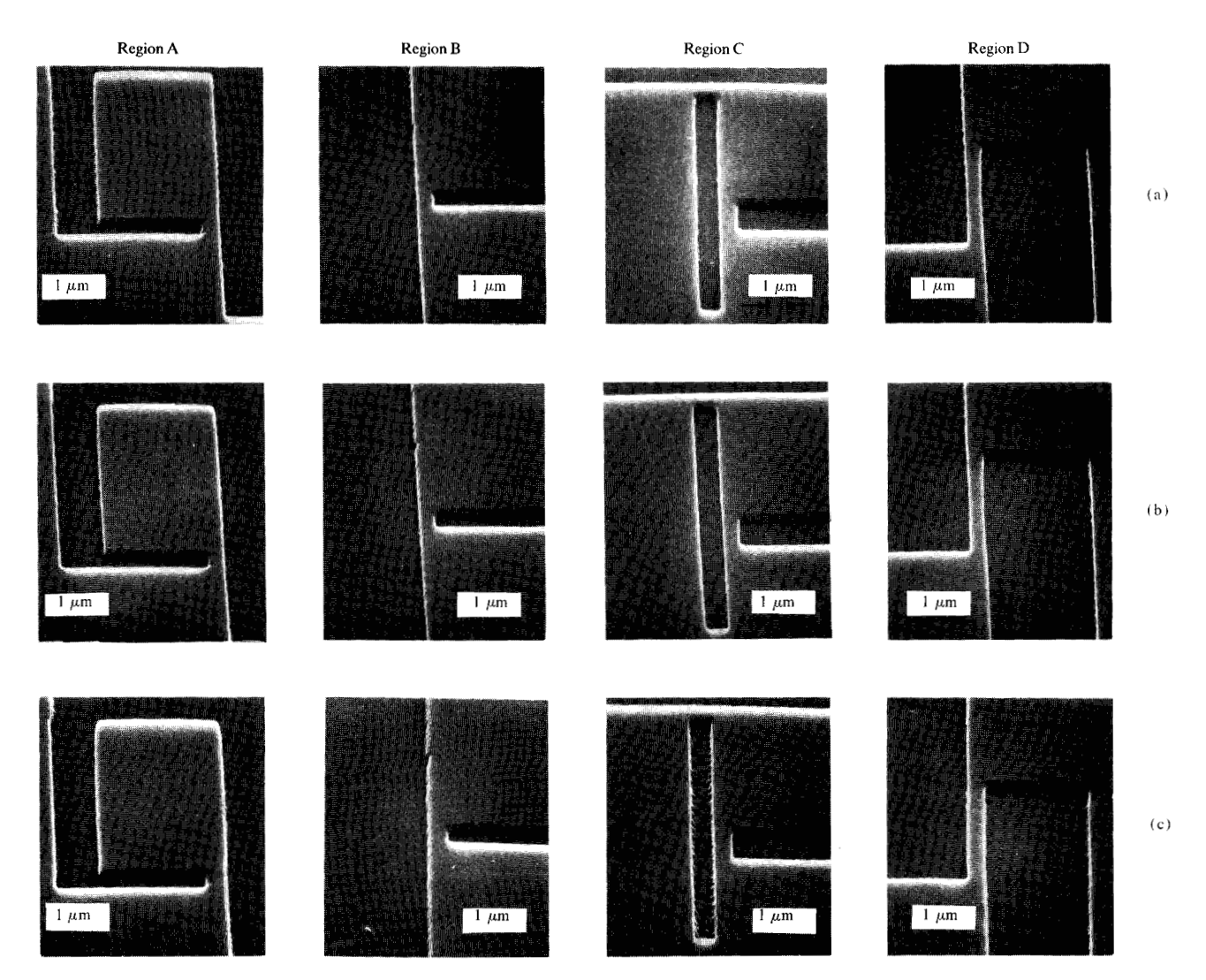


Figure 3 Scanning electron micrographs (SEMs) of the four regions noted in Fig. 2 under three different conditions: (a) Uncorrected pattern. (b) Corrected pattern with eight rectangles, each exposed with relative incident electron exposures as noted in Fig. 2. (c) Corrected partitioned pattern with 21 rectangles, each exposed with relative exposures as noted in Fig. 5b. See text for discussions on the micrographs. Note in all cases that the micrographs have been taken with a tilt of $\approx 50^{\circ}$, leading to an apparent foreshortening along the y axis.

through the use of the self-consistent algorithm can be summarized as follows. Proximity corrections are attempted on a given pattern (e.g., the eight rectangles in Fig. 2). The quality of corrections attainable with the given pattern is then assessed on the basis of an algorithm (discussed below). If the pattern quality fails to satisfy certain criteria, the pattern is subdivided as needed. Finally, proximity correction is reattempted on this partitioned pattern. In principle, this procedure can be repeated until the pattern quality criteria are satisfied or until it becomes impossible to further subdivide the pattern on the basis of physical limitations of the e-beam machine.

The algorithm for assessing pattern quality and for subsequent pattern partitioning was described briefly in Ref. [5]. The algorithm first defines "sample" points and "associated" areas. Figure 5(a) shows one definition of sample points used for the pattern in Fig. 2. While the density and relative location of the sample points are inputs to the algorithm, some constraints need to be imposed to prevent sample points from being too close (or the associated areas too small) when compared to either the beam diameter of the e-beam machine or the extent of forward scattering β_f of the proximity function [1]. Generally we use, for 1- μ m lithography, nominal sample point spacings of \approx 6 μ m (or less), each with a nominal associ-

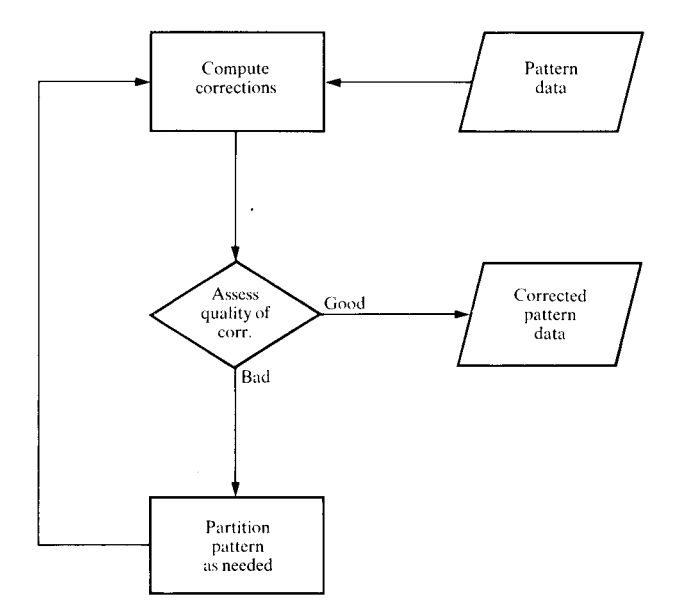


Figure 4 Flowchart depicting the strategy for automatic partitioning of patterns within the self-consistent technique.

ated area with dimensions of $6 \mu m$ (or less) length and $1 \mu m$ width. The quantity ε is then calculated at each sample point *i*. This quantity [1] is a measure of the magnitude of the proximity effect at a point r_i due to the writing of a pattern consisting of m shapes (each with area A.):

$$\varepsilon(r_i) = \sum_{J=1}^m n_J \int_{A_J} f(r_{ij}) dA_J, \tag{1}$$

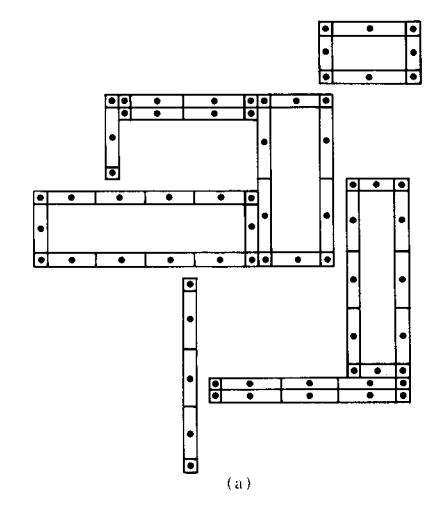
where $r_{ij} = |\mathbf{r}_i - \mathbf{r}_j|$, n_J is the incident electron exposure for shape J, and f is the proximity function [1]. The parameters used throughout this work are $\beta_f = 0.1 \ \mu m$, $\beta_b = 2.5 \ \mu m$, and $\eta_E = 0.9$, as suggested in Ref. [1]. The quantity ε can be separated into two parts. One part reflects the influence on the sample point i of the very shape in which that sample point i belongs, i.e., the *intrashape* contribution. This can be written as

$$\varepsilon_{A}(r_{i}) = n_{I} \int_{A} f(r_{ij}) dA_{I}. \tag{2}$$

The second part, i.e., the intershape contribution, can be written as

$$\varepsilon_{\rm p}(r_i) = \varepsilon(r_i) - \varepsilon_{\Lambda}(r_i). \tag{3}$$

For each sample point, two measures of the degree of "residual" proximity are defined: $k_1(i)$ and $k_2(i)$. These can also be interpreted as the criteria by which the quality of the pattern can be judged. The quantity k_1 is related to the deviations within a given shape due to proximity effect from neighboring shapes. We define



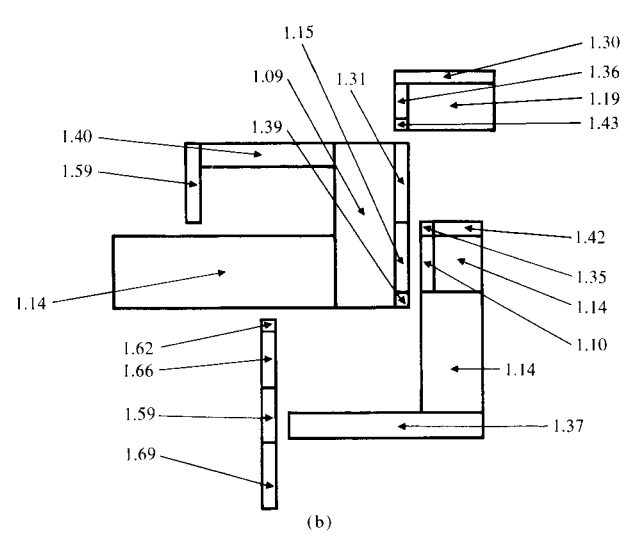


Figure 5 (a) Pattern (shown in Fig. 2) with sample points (①) and associated rectangular areas. (b) Partitioned pattern with 21 rectangles that is obtained using the algorithm described in the second section of this paper. Incident electron exposure values for each of the 21 rectangles, computed using the self-consistent algorithm, are noted.

$$k_{1}(i) \equiv \frac{\varepsilon_{R}(i)}{\sum_{i=1}^{n_{p}} \varepsilon_{R}(i)/n_{p}},$$
(4)

where $n_{\rm p}$ is the number of sample points in shape I, and the quantity in the denominator of Eq. (4) is the average value of $\varepsilon_{\rm R}$ in that shape. The quantity $k_{\rm 2}(i)$ is defined to be the ratio of the intershape to intrashape contributions at a point i. Thus,

$$k_{\rm p}(i) \equiv \varepsilon_{\rm p}(i)/\varepsilon_{\rm A}(i).$$
 (5)

A point *i* can be deemed to be suffering from excess residual proximity effect if

$$k_1(i) > k_1^c \text{ and } k_2(i) > k_2^c,$$
 (6)

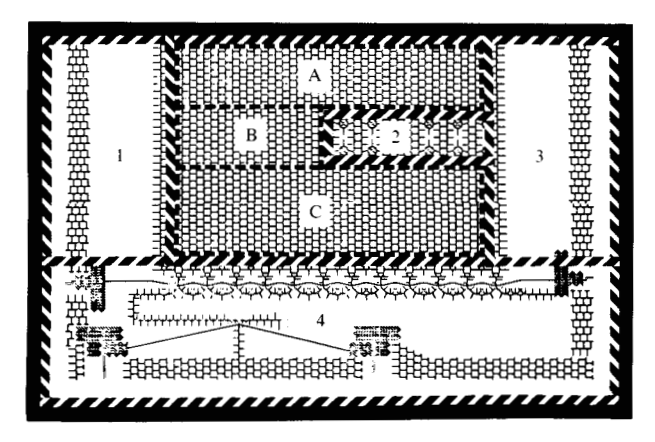


Figure 6 Zoning of an electron lithographic pattern into four Azones (i.e., 1, 2, 3, and 4) and three H-zones (i.e., A, B, and C) (reprinted with permission from Ref. [3b]).

Table 1 Assignments of shapes in Fig. 7 to S-zones and frames.

Shape	S-zone index		
	(I-I,J)	(I, J)	(I+I,J)
	Origin	al Pattern	
A	Frame	Frame	Frame
В	S-zone	_	_
C	S-zone	Frame	_
D	S-zone	Frame	_
E	_	S-zone	Frame
F	_	S-zone	Frame
G	_	S-zone	Frame
H	_	Frame	S-zone
I	_	_	S-zone
J	-		Frame
	Partitio	ned Pattern	
A1	S-zone	Frame	_
A2	Frame	S-zone	Frame
A3		Frame	S-zone
В	S-zone	_	_
C	S-zone	Frame	_
D	S-zone	Frame	
E	_	S-zone	Frame
F1	_	S-zone	Frame
F2	_	Frame	S-zone
G		Frame	S-zone
H	_	Frame	S-zone
I	-		S-zone
J	-	_	Frame

where k_1^c and k_2^c are constants chosen to define the extent of pattern partitioning. In such a case, the associated area corresponding to the sample point i is partitioned. Note, however, that a sample point is not partitioned if its associated area lies next to another area that belongs to an-

other shape. Thus, a given shape is partitioned as a collection of shapes equal to the sum of the associated areas [whose sample points meet the criteria of Eqs. (6)] and the minimum number of rectangles that fill the remaining area of the shape. An appropriate choice of the parameters k_1^c and k_2^c can lead to the *minimum* amount of partitioning necessary to attain the desired level of proximity corrections for particular lithographic conditions.

Implementation of the above algorithm on the pattern shown in Fig. 2 yields the partitioned pattern shown in Fig. 5(b). The values of k_1^c and k_2^c used were 1.5 and 0.2, respectively. These values have the following physical interpretation. A value of $k_1(i) > 1.5$ implies that the intershape contribution [Eq. (3)] at the sample point i exceeds the average intershape contribution to that shape by 50%. A value of $k_2(i) > 0.2$ implies that at the sample point i, the intershape contribution is greater than 20% of that for the intrashape contribution [Eq. (2)]. The calculated values of exposure n_I using the self-consistent algorithm on the 21 shapes are also noted in Fig. 5(b).

The increased quality of corrections attained through judicious pattern partitioning is evident in the SEM micrographs in Fig. 3(c). Note in Fig. 3(c) the essential absence of any bulging (see region C) or narrowing of the resist gap (see region D). Finally, it is worth noting that a significant strength of this technique is its ability to partition the pattern only where needed and as determined by the criteria based quantitatively on the magnitude of the proximity effect.

Partitioning for efficient computation

Zoning schemes have been devised [3b] to make the self-consistent computation more efficient. Zones are defined to be regions of a pattern (Fig. 6) where the pattern is either explicitly periodic in two dimensions (such regions are called *H-zones*) or without any explicit periodicity (*Azones*). A small region within an A-zone is used [3b] to compute corrections to the repeating pattern unit. Results are associated with the rest of the periodic array. Regions within an A-zone are subdivided into rectangular regions called *S-zones*. Shapes that lie within an S-zone and within a *frame* (a border surrounding the S-zone) are used in the self-consistent computation.

Figure 7(a) shows ten shapes that lie in and around a hypothetical S-zone with indices (I, J) inside a certain A-zone. The assignment of shapes to S-zones and frames of S-zones is shown in the *Original Pattern* section of Table 1. Note that shapes A and J are so extensive that they are assigned to some S-zones beyond the geometrical limits of Fig. 7(a). All the other shapes can be assigned to any one of the three S-zones noted in the table. Note that for

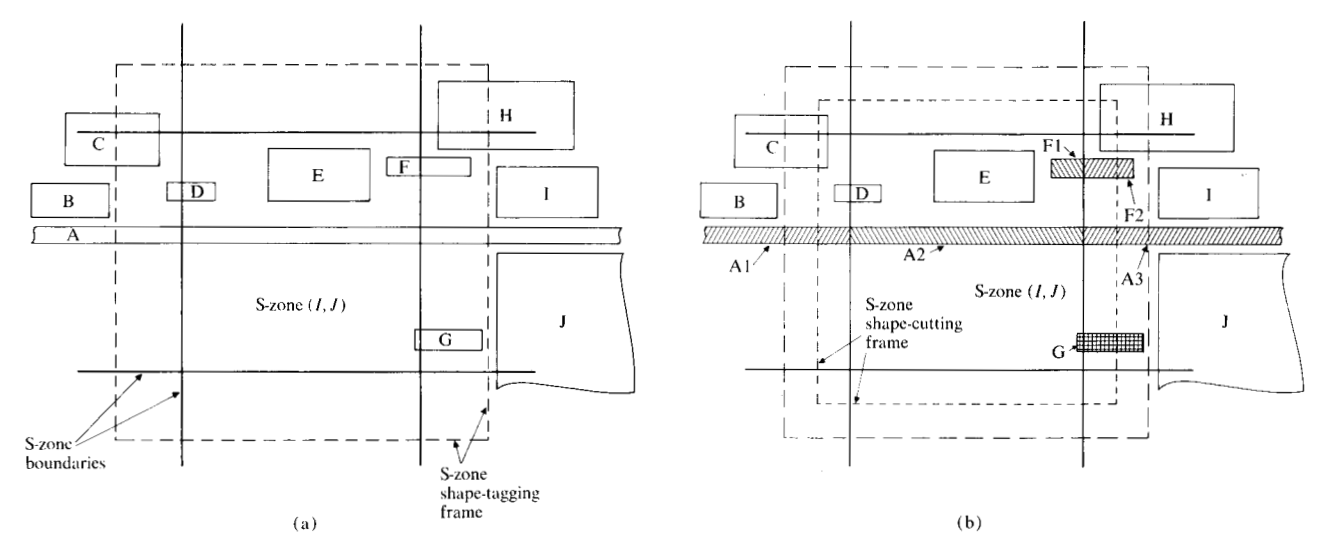


Figure 7 (a) Ten shapes that lie in S-zones and frames as noted in Table 1 in the *Original Pattern* section. (b) Corresponding thirteen shapes obtained after partitioning according to the algorithm in the third section of this paper. Assignments of shapes to S-zones and frames are given in Table 1 in the *Partitioned Pattern* section.

the sake of simplicity in the following discussion, we restrict our attention to only three S-zones along the x axis [i.e., those with indices (I-1, J), (I, J), and (I+1, J)] and ignore the S-zones along the y axis [i.e., those with indices (I, J+1), etc.]. Clearly, all of the algorithms and conclusions presented below are equally applicable to S-zones along the y axis. Consider now the seven shapes that would be used in the self-consistent solution of the shapes in the S-zone (I, J). Since shapes B, I, and J are not included in the computation, the mutual interactions between them and the long shape A are incorrectly ignored. In addition, the interaction between shapes G and J is ignored; this can lead to serious errors in the computed exposure values for shape G.

A solution to these problems can be obtained by "cutting" some shapes into smaller ones so that more accurate exposure values can be computed for the component pieces. The algorithm for cutting shapes involves first defining a shape-cutting frame [see Fig. 7(b)] that circumscribes an S-zone. Next, one stipulates the cutting into two pieces of those shapes belonging to an S-zone but extending beyond that S-zone's shape-cutting frame. The shape is cut, if necessary, at the S-zone boundary. Finally, one prevents "sliver" shape formation (for example in the case of shape G) by reassigning the entire shape to the neighboring S-zone, rather than cutting it. The application of these rules to the ten shapes in Fig. 7(a) results in the thirteen shapes shown in Fig. 7(b).

Examination of the assignments (listed in Table 1 in the *Partitioned Pattern* section) shows that computations in

S-zone (I-1, J) take into account proper interactions between shapes A1 and B, while computations in S-zone (I+1, J) take into account proper interactions among shapes A3, J, and G. Finally, note that reassignment of shape G to S-zone (I+1, J), in order to prevent the formation of a sliver shape in S-zone (I, J), also properly accounts for the mutual interaction between it and shape J.

SPECTRE

A new version of SPECTRE (for Self-consistent Proximity Effect Correction Technique for Resist Exposure), with an architecture similar to the earlier version [2, 3c], has been created that includes the previously described algorithms. Figure 8 shows the flowchart of the programs that comprise SPECTRE. As before, the program is initiated via an interactive program (SPECREAD) that prepares and checks input parameters regarding electron lithographic and pattern conditions to be used for proximity correction. An arbitrary pattern is divided into various zones [3b] (via the program ZONMAP) on the basis of whether the proximity corrections are to be performed on all shapes (if the pattern is nonrepeating) or only on some (if the pattern is repeating). In the latter case, the computed values are associated with the rest of the repeating pattern. A program (WINDOW) separates the pattern data into two parts: one with the pattern data (COMP. SHAPES, abbreviated as CS) that are to be explicitly used for proximity computations; the other with the pattern data (ASSOC. SHAPES) that are part of the repeating pattern and that are only to be associated with the computed corrections. The CS pattern data are next processed by three programs. The program ZONTAG tags

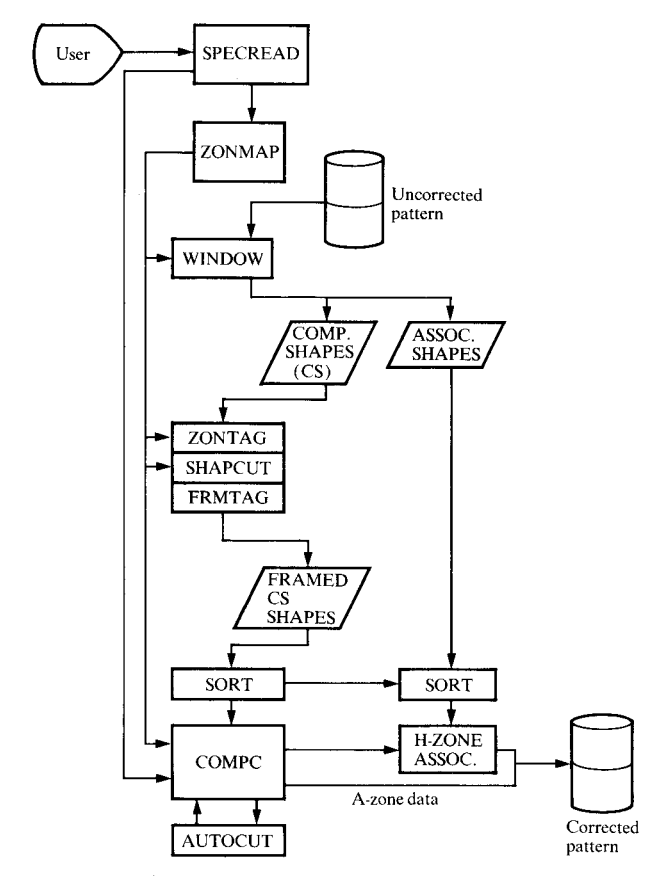


Figure 8 Flowchart of SPECTRE. See text for explanation of individual programs.

the pattern according to zones, as described previously [3b]. By using the algorithm described in the last section, shapes that traverse zone boundaries are subdivided by the program SHAPCUT. The program FRMTAG replicates and tags shapes if they belong in the frames of zones, as reported previously [3b]. After a SORT, to arrange pattern data sequentially by zones, the computation of corrections is performed by the program COMPC. By using the self-consistent algorithm and the algorithm described in the second section of this paper, the program automatically subdivides shapes and recomputes corrections in the pattern via the program AUTOCUT.

Conclusion

This work has demonstrated that prudent partitioning of the pattern data can lead to significant enhancements in the quality of proximity effect corrections using the selfconsistent algorithm.

An algorithm has been developed that, by using the magnitude of the proximity effect at sample points throughout the pattern, automatically subdivides *only* those regions of a pattern wherein certain criteria are not

met. The subdivided pattern is subsequently proximity-corrected using the self-consistent algorithm. Experimental results show an improvement in the quality of corrections.

Another algorithm has been developed that subdivides shapes that traverse or significantly extend beyond zone boundaries. Such an algorithm has been shown to take into account the proper interaction of intershape proximity effects between shapes in adjoining zones.

Acknowledgment

The experimental aspects of this work were made possible by the skilled assistance of V. E. Hanchett and A. J. Kraft of the IBM Research Division laboratory in San Jose, California.

References

- Mihir Parikh, "Proximity Effects in Electron Lithography: Magnitude and Correction Techniques," IBM J. Res. Develop. 24, 438 (1980).
- Mihir Parikh, "SPECTRE—A Self-Consistent Proximity Effect Correction Technique for Resist Exposure," J. Vac. Sci. Technol. 15, 931 (1978).
- 3. Mihir Parikh, "Corrections to Proximity Effects in Electron Beam Lithography. (a) I. Theory, (b) II. Implementation, and (c) III. Experiment," J. Appl. Phys. 50, 4371, 4378, and 4383 (1979).
- W. D. Grobman, A. J. Speth, and T. H. P. Chang, "Proximity Correction Enhancements for 1-μm Dense Circuits," *IBM J. Res. Develop.* 24, 537 (1980, this issue).
- M. Parikh, "Technique for Automatic Subdivision of Pattern Data for Enhanced Proximity Effect Corrections," IBM Tech. Disclosure Bull. 21, 4278 (1979).
- N. D. Wittels and C. I. Youngman, "Proximity Effect Correction in Electron-Beam Lithography," Proceedings of the Eighth International Conference on Electron and Ion Beam Science and Technology, Seattle, WA, 1978; R. Bakish, Ed., The Electrochemical Society, Princeton, NJ; p. 361.
- Naoshi Sugiyama, Naoaki Aizaki, Akira Kawagi, and Yasuo Tarui, "A Data Processing System for Electron Lithography," Ref. 6, loc. cit., p. 184.
- 8. J. H. C. Phang and H. Ahmed, "A New Proximity Effect Correction Method for Accurate Pattern Fidelity," *Pro*ceedings of Microcircuit Engineering 79, Sept. 1979, Institute of Semiconductor Electronics, Aachen, Germany, in press.
- T. H. P. Chang, W. D. Grobman, and A. J. Speth, "Partitioning E-Beam Data for Proximity Corrections," *IBM Tech. Disclosure Bull.* 20, 3809 (1978).
- C. H. Ting, R. L. Anderson, D. Y. Saiki, and A. J. Kraft, "Chrome Mask Fabrication with Electron-Beam Lithographic System," J. Vac. Sci. Technol. 15, 948 (1978); C. H. Ting, A. M. Patlach, A. J. Kraft, and P. R. Jaskar, "Mask Fabrication with Vector Scan Electron Beam System," SPIE 174 (Developments in Semiconductor Microlithography IV), 90 (1979).

Received April 24, 1980

Mihir Parikh is located at the IBM Research Division laboratory, 5600 Cottle Road, San Jose, California 95193; Donald E. Schreiber is now at the law offices of Thomas E. Schatzel, 3211 Scott Boulevard, Santa Clara, California 95050.